

# A Practical Procedure to Analyze Singular Configurations in Closed Kinematic Chains

Oscar Altuzarra, Charles Pinto, Rafael Avilés, and Alfonso Hernández

**Abstract**—The authors present a general method for the automated singularity analysis of any mechanism at a given configuration. The procedure uses a base of the motion space. This is obtained from a velocity equation characterized by a geometric matrix. This special form of Jacobian matrix has some advantages for automatic implementation. This approach provides the degree of freedom associated with the singularity, uncontrolled motion, and kinematic dependencies. It also facilitates the choice of actuators and redundant devices. The method has been implemented in a computer program for kinematic analysis.

**Index Terms**—Constraint singularity, geometric matrix, parallel manipulators, singular configurations, velocity equation.

## I. INTRODUCTION

SINGULARITY analysis in mechanisms is a very active research field. Related issues, such as mobility analysis in single closed-loop and one degree-of-freedom (DOF) linkages [1], [2], have been studied already. The singularity problem in serial manipulators has been analyzed and solved [3], [4]. In [5]–[9], singular configurations in parallel manipulators and hybrid-chain manipulators have been obtained. Even a unified approach to the singularity analysis of redundant input–output devices [10] has been proposed. At present, singular configurations are still being identified as it is the case of the so-called constraints singularities [11]. It is widely assumed that this line of research has not yet reached its maturity.

In recent times, several classifications of singular configurations have been issued, some of which should be noted in particular: Ma and Angeles [12] typify architecture, configuration, and formulation singularities; Notash [13] divides them in branch degeneracy and uncertainty configuration; and Park and Kim [14] propose configuration space singularity, actuator, and end-effector singularities. Nevertheless, in our view, three classifications could be highlighted. The first is that proposed by Hunt [15]. In this magnificent text, the basic concepts to define a singular configuration are established. This apparently simple classification into stationary and uncertainty configurations covers every recent variation. The second is from Gosselin and Angeles [16] and uses the input–output implicit function to

provide two Jacobian matrices [A] and [B]. Mathematical singularity of those matrices leads to three types of physical singularities. In the third [17], Zlatanov *et al.* propose a more detailed classification of singularities into six different types [redundant input (RI), redundant output (RO), impossible input (II), impossible output (IO), increased instantaneous mobility (IIM), and redundant passive motion (RPM)]. In this paper, a classification of singularities is also proposed. The object of this classification is not to put forward new types but to adequate them to the analysis method that will be explained later.

To detect and/or analyze singular positions, symbolic computation has been used only in particular parallel robots, and algebraic methods seem quite limited. Some authors propose methods based on the degeneracy of the screws [18]. These are similar to another method based in the Grassmann (or line) geometry [19]. Another alternative is that proposed by Park and Kim [14], in which Riemannian geometric formulation is employed to characterize a singularity as a dimensional change in manipulability.

Numerical methods, on the other hand, even being easily automated, have difficulties finding all singular positions in the workspace. Regarding strategies to find every singular configuration in any manipulator, in [20] a general algorithm is presented. This is capable of automatization, although some of its phases would require a deep knowledge of the specific linkage analyzed.

Each of these methods are based on the Jacobian matrix of the position equations. Hence, this background should not end without a reference to Freudenstein [21] that laid the basis of these approaches.

Nevertheless, the authors believe that there is still much research to be done. The contents of this paper do not intend to solve every existing unknown but to contribute with a valid tool to understand the kinematic behavior in singular positions. The method proposed will help to design parallel manipulators, providing a tool for the singularity-free path planning.

The procedure presented in this paper is valid for open, closed, or hybrid kinematic chains and redundant or nonredundant manipulators. This is because the approach chosen is independent of the choice of inputs and outputs.

The structure of the paper is as follows. In the second section, the velocity equation used is explained. A very specific Jacobian matrix called the geometric matrix is used. Its choice is due to some good characteristics for singularity analysis. In Section III, a simple classification of singularities is presented. They are defined and briefly compared with other classifications already referenced. In Section IV, the method for analysis of a given configuration is explained for the different types of singularities. It is

Manuscript received November 3, 2003; revised February 26, 2004. This paper was recommended for publication by Associate Editor G. Oriolo and Editor I. Walker upon evaluation of the reviewers' comments. This work was supported in part by the Spanish Government via Ministerio de Ciencia y Tecnología under Project DPI2002-04580-C02-01 and in part by the University of the Basque Country under Project 9/UPV00145.345-14494/2002.

The authors are with the Department of Mechanical Engineering, School of Engineering of Bilbao, University of the Basque Country, Alameda de Urquijo s/n Bilbao 48013, Spain (e-mail: impalmaa@bi.ehu.es; imppicac@bi.ehu.es; impavgor@bi.ehu.es; imphefra@bi.ehu.es).

Digital Object Identifier 10.1109/TRO.2004.832798

based in the vectors that form a basis of the null-subspace of the geometric matrix. In Section V, a numerical method for the detection of singular positions is proposed. Up to now, this method has some limitations, as it only detects singular positions in the path followed by the manipulator inside the workspace. To do that, the first nonzero eigenvalue and the determinants associated with the dependable kinematic parameters are used as indexes. Its advantages are that it is an easily automated method, fast in computational terms, and valid for any manipulator's topology. In Section VI, we present a brief discussion on the possibilities of applying this procedure for the singularity mapping.

## II. VELOCITY EQUATION

An element of a mechanism may be modeled with two nodes in planar cases and three in spatial ones. Differentiation of the rigid body condition on the node coordinates produces a velocity equation of the form [22]

$$[g]_e \{\dot{x}\}_e = \{0\} \quad (1)$$

where  $\{\dot{x}\}_e$  is the vector containing the components of the nodal velocities in the element  $e$ , and  $[g]_e$  is called the geometric matrix of the element  $e$ . This matrix has the data related to link orientation but it is independent of its length, section, or other mechanical properties. If the mechanism is modeled with  $M$  elements and  $n$  nodes, the velocity (1) of every one of the  $M$  elements may be expanded to the dimension of the total number of components of the  $n$  nodes

$$[\bar{g}]_e \{\dot{x}\} = \{0\} \quad (2)$$

where  $\{\dot{x}\}$  is the vector containing the components of the nodal velocities in the mechanism, and  $[\bar{g}]_e$  is the geometric matrix of the element  $e$  expanded to the complete dimension. Assembling the matrices of all the elements provides the geometric matrix  $[G]$  for the complete mechanism

$$[G] = \sum_{e=1}^M [\bar{g}]_e. \quad (3)$$

Kinematic pairs are introduced through the conditions with which nodal velocities have to comply. For example, nodes are merged in revolute pairs in planar mechanisms and spherical ones in spatial linkages as linear velocities are equal. Finally, the velocity equation for the complete mechanism may be expressed as

$$[G]\{\dot{x}\} = \{0\} \quad (4)$$

and provides the solution of kinematic analysis for velocities.

In the Appendix, application of the geometric matrix to the four-bar linkage is presented to show the ease of this approach and its ability to be automated for any mechanism. In the case of planar mechanisms with only revolute pairs or spatial mechanisms with spherical ones, the geometric matrix is independent of the dimensions of the linkage. Nevertheless, the effect that special dimensions have in singular positions is considered through the corresponding orientations.

The geometric matrix is, in fact, a particular case of Jacobian matrix. The geometric matrix has some advantages in relation

to singularities that will be shown in the following sections. For example, it is homogeneous, the finding of the DOF in a singular position is direct, and the method facilitates the choice of actuators.

## III. CLASSIFICATION OF SINGULARITIES

A definition for singularity has been often stated from the point of view of the mathematic impossibility in solving the kinematic problem in certain positions [12], [14], [16], [20], [23]. Nevertheless, any definition for singularity has a physical notion. A singularity occurs whenever there is an instantaneous or permanent, global, or local alteration of the full-cycle mobility, leading to either the blockage or the loss of control of some link. In that sense, the authors propose two singular situations: when there is an increase in the full cycle mobility and when there is some unexpected dependency among kinematic parameters in the linkage. The first kind of singularity is widely accepted in the sense given here. Regarding the second one, it is a generalization of the concept that involves the different types already defined in the references, such as stationary configuration [15] or RI, RO, IO, II [17].

### A. Increased Mobility Configuration

First, a singularity occurs when the full-cycle mobility  $F$  of the mechanism is increased, and as a consequence, the motion of the mechanism as a whole is altered. In this paper, the increased mobility (IM) singularity is proposed in the same terms than the configuration space singularity proposed by Park and Kim [14], and the IIM by Zlatanov *et al.* [17]. In a practical sense, the IM requires additional inputs to define the motion in that position whether other types will require a change in the choice of inputs. In addition, it should be mentioned that this type of configuration is instantaneous, but may be chained to adjacent IM poses acquiring apparently a permanent nature.

### B. Dependent Kinematic Parameters Configuration

In a mechanism, there are independent kinematic parameters that completely define its motion in a nonsingular configuration. Those kinematic parameters can be identified as derivatives of the generalized coordinates and are chosen in sets of, for example, module of the angular velocity or nodal velocity.

A singularity of this type occurs when, due to the specific configuration of the mechanism, an unexpected dependency exists among some of the full-cycle independent kinematic parameters. This is called a dependent kinematic parameter (DKP) configuration. Such an occurrence suggest a change in the location of the DOF in the mechanism affecting locally some parts of the linkage, such as the input or the output.

A linkage provides a motion as a function of  $F$  independent kinematic parameters; therefore one expects to get equations that relate  $r$  kinematic parameters, being  $r$  greater than  $F$ . For example, in the 3-RRR planar platform in Fig. 1, equations could be obtained relating angular velocities of links  $\omega_i$  weighted with  $\gamma_i$  coefficients as follows:

$$\gamma_1\omega_1 + \gamma_2\omega_2 + \dots + \gamma_r\omega_r = 0. \quad (5)$$

When such a relationship may be found among  $r = F$  kinematic parameters with full cycle independence, some singularity

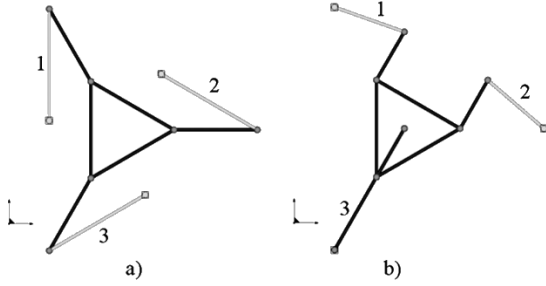


Fig. 1. The 3-DOF linkages in DKP configuration (a)  $r = F$  and (b)  $r < F$ .

is affecting the linkage. A finite number of sets of such kinematic parameters are chosen to check their independency, i.e., inputs and outputs.

1) *DKPs in the Input*: The fact that there exists some dependence among the possible inputs implies that there is a possibility of motion in the mechanism when those inputs are null. In that sense, the output gains some DOF. For example, in the case in Fig. 1(a) the relationship among the links (1, 2, 3) with fixed  $R$  pairs is

$$\omega_1 + \omega_2 + \omega_3 = 0. \quad (6)$$

The same considerations may be done when there exist equations like (5) with  $r < F$  kinematic parameters, as is the case of the configuration shown in Fig. 1(b) where an equation relating angular velocities of the links (1, 2) with fixed  $R$  pairs is found:

$$\omega_1 - \omega_2 = 0. \quad (7)$$

These configurations correspond to type 2 in the classification proposed by Gosselin and Angeles, and II singularities (and RO or RPM, depending on where is the uncontrolled motion) in Zlatanov's.

2) *DKPs in the Output*: If the kinematic parameters considered are the ones defining the desired output, an analogous analysis may be performed using nodal velocities, angular velocities, or joint velocities. In that case, DKP configuration corresponds to a type 1 and IO configuration.

3) *Link Impossible Motion*: The limit to those relationships is  $r = 1$ , where an independent kinematic parameter is null whatever inputs given. Upon evaluation of the kinematic parameters that define completely the velocity of a link, if all of them are included in equations of this type, the link will have lost its capacity for motion. This configuration is called link impossible motion (LIM). This may occur in input, output, or passive links. The last case may not show a practical advantage when analyzing the motion of the input or output but it could influence operations such as calibration or redundant sensing. An example is given in the 3-RRR linkage in Fig. 2, where the link with fixed  $R$  pair on the right is motionless.

It may also occur that a group of  $r$  independent kinematic parameters are related through more than one equation. Moreover, it can be noted that configurations with DKPs may be found in increased mobility configurations.

This approach may be also used to determine the DOF of the gripper in a parallel manipulator. This is useful to detect constraint singularities. A study of dependencies among the kinematic parameters that define the motion will indicate how many are independent and therefore the DOF.

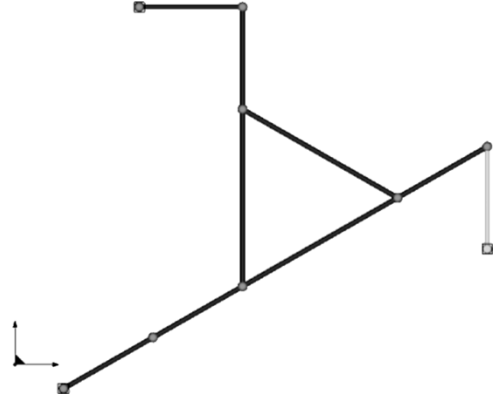


Fig. 2. The 3-DOF mechanism in DKP configuration  $r = 1$ .

#### IV. METHOD FOR SINGULARITY DETECTION

The geometric matrix provides the feasible motions of the linkage (the null-space of  $[G]$ ) referred to as the motion space [24]. Its dimension is the instantaneous DOF of the linkage in a given configuration. Equation (4) is a particular case of the following equation when the value of  $\lambda$  is null:

$$[G]\{\dot{x}\} = \lambda\{\dot{x}\}. \quad (8)$$

The  $L$  eigenvectors  $\{v_j\}$ , corresponding to the null value of  $\lambda$ , are linearly independent and constitute a basis for the subspace of  $L$  dimensions. This subspace of a vector space with dimensions of the matrix  $[G]$  forms the space of possible motions of the mechanism. Any vector representing a motion of the mechanism is a linear combination of those vectors. Instantaneous nodal velocities are expressed by the following equation in matrix form:

$$\{\dot{x}\}_{D \times 1} = \sum_{j=1}^L \beta_j \{v_j\}_{D \times 1} = [V]_{D \times L} \{\beta\}_{L \times 1}. \quad (9)$$

This equation provides a relationship between all components of nodal velocities in the vector  $\{\dot{x}\}$  (planar  $D = 2n$ , spatial  $D = 3n$ ) and the  $L$  eigenvectors  $\{v_j\}$  weighted with  $\beta_j$  terms, where  $L$  is the instantaneous DOF. Matrices  $[V]$  (formed in columns by the eigenvectors) and  $\{\beta\}$  give a compact expression.

In some cases, it is more common to use the angular velocity of the links. Then, an expression is found relating the components of the angular velocities of the  $M$  links to the nodal velocities, using the velocity field

$$\{\omega\}_{C \times 1} = [\Omega]_{C \times L} \{\beta\}_{L \times 1} \quad (10)$$

where  $\{\omega\}$  is the vector of components of angular velocities (planar  $C = M$ , spatial  $C = 3M$ ), and  $[\Omega]$  is the matrix with the coefficients that relate components and the  $\{\beta\}$  terms in (9). Expressions with joint velocities can be found easily. In planar mechanisms, subtracting in (10) the corresponding rows of the angular velocities of the links that come to the joint, and in spatial ones, the components. If angular as well as linear velocities are to be considered in the analyses, a total or partial combination of (9) and (10) can be used.

All of these systems of equations are the tool to identify and classify the singularities proposed in the previous section.

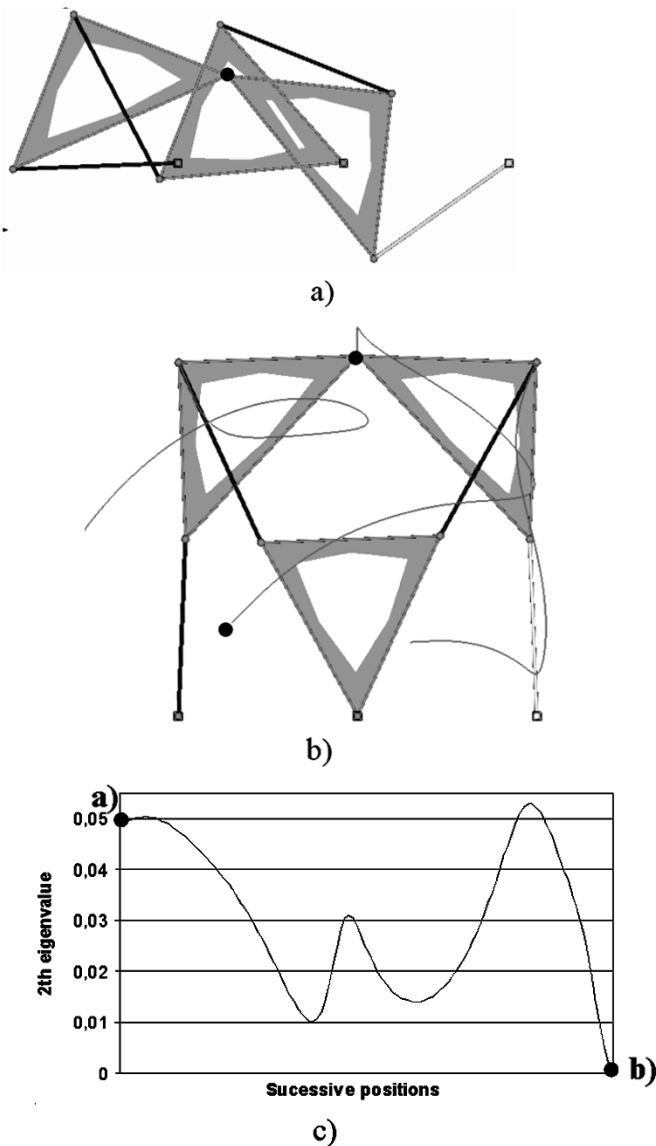


Fig. 3. Double butterfly mechanism moved to an IM configuration and the plot indicating IM proximity.

#### A. IM Configuration

IM singularity existence is detected in the instantaneous DOF. As this is coincident with the number of null eigenvalues, the proximity of the first nonzero eigenvalue to null indicates the proximity to IM singularity. In the software developed by this research team, the motion of the linkage is simulated using finite displacement analysis. The geometric matrix is found for every configuration reached, and the null eigenvalue problem is solved. The number of null eigenvalues  $L$  indicates the instantaneous DOF. In a nonsingular position is equal to the full-cycle mobility  $F$ . A plot of the variation of the first nonzero eigenvalue along the motion is produced. In Fig. 3, a 1-DOF linkage is moved from (a) a nonsingular position to (b) an IM configuration. In Fig. 3(b), the paths of three nodes have been plotted, and the graph in Fig. 3(c) shows the variation of the second eigenvalue toward a null value.

Once an increment in  $F$  is detected, upon evaluation of the rank deficiency of the geometric matrix, a deeper analysis is car-

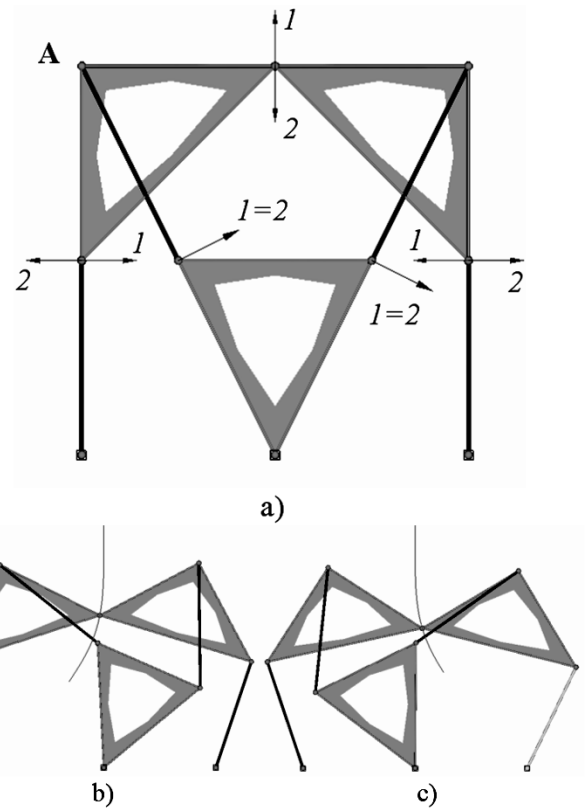


Fig. 4. Vectors of the motion space and the two different possibilities of motion after IM.

ried out. The increment in the DOF of the linkage implies the existence of uncontrollable motion in the mechanism. Such a position is usually avoided, but it can also be surpassed with additional inputs (either redundant inputs or locking devices). From a theoretical perspective, the uncertainty positions are points of bifurcation in the path. Therefore, it is quite interesting to analyze the possibilities of motion from that position. In that field, vectors of the null subspace play a major role.

In the example of Fig. 4(a), the two vectors of the motion space are found as the two eigenvectors corresponding to a null eigenvalue. The two different motions may be found upon linear combination of both vectors and provide the two branches of the path from that position. A further examination of those vectors indicates that, in this example, the instantaneous center of rotation of the coupler in both possible motions is in the same point  $A$ . This causes the branches to be tangent in the double point. In Fig. 4(b) and (c), the linkage is shown in the two different branches. In Fig. 5, the path of the revolute pair already mentioned is plotted, showing the existence of two other points of bifurcation, and therefore, IM configurations.

To analyze the possible motion when  $F$  inputs are locked, (9) and (10) are used.  $F$  equations corresponding to the null inputs are extracted from those expressions. This system of  $F$  equations in  $L$  unknowns (the  $\{\beta\}$  terms) has infinite solutions.  $L$  minus  $F$  terms  $\beta_j$  are selected and the rest are expressed as a function of them. A proof value to these will provide different solutions to  $\{\beta\}$  and, upon substitution in (9) or (10), the uncontrollable motions.

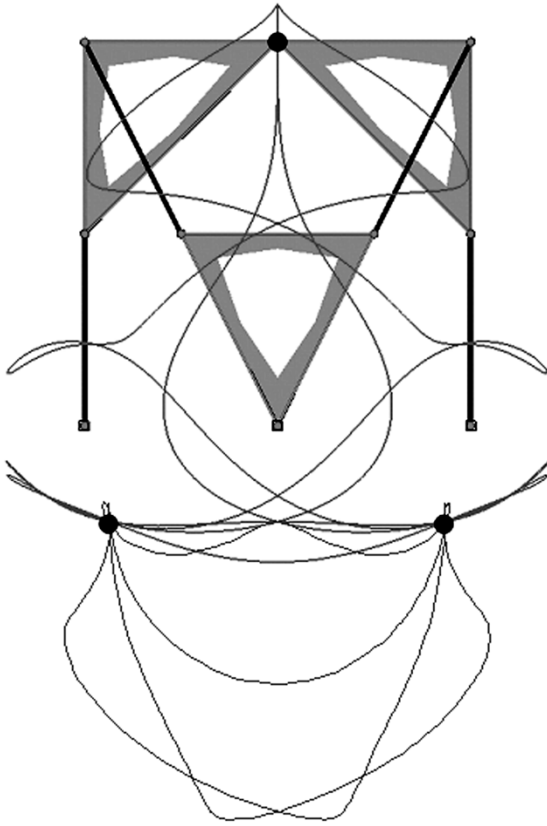


Fig. 5. Path of the upper  $R$  pair with three bifurcation points (black dots).

For example, if working exclusively with angular velocities, the extracted system of equations would be

$$\{\omega_{\text{input}}\}_{Fx1} = \{0\} = [\Omega_i]_{FxL} \{\beta\}_{Lx1} \quad (11)$$

where  $\{\omega_{\text{input}}\}$  is the vector with the  $F$  input rotations,  $[\Omega_i]$  is the matrix with the correspondent rows from matrix  $[\Omega]$ , and  $\{\beta\}$  are the  $L$  terms. In the example of Fig. 5,  $F = 1$  and  $L = 2$ , one of the terms is found as a function of the other. A proof value of 1 will give the uncontrollable form of the motion.

In spatial mechanisms, a branching of the configuration space lately called constraint singularity [11] can also be analyzed with this approach. The DOF of the platform could be found searching for the independency of the kinematic parameters that define its motion, i.e., the components of the nodal velocity of a point in the platform and the components of the angular velocity.

### B. DKP Configuration

The DKP configuration of a mechanism is detected again using a system of equations extracted from either (9) or (10) or even a combination of them. Sets of  $F$  kinematic parameters are chosen to perform an analysis of their independency. This choice has to be done carefully, as kinematic parameters that could define the motion completely are needed.

In this way, an analysis of the selected input links or platform kinematic parameters may be performed, but it is also possible to perform a wider analysis to check dependency among every link in the mechanism in order to choose the more interesting links to be the input(s) or output(s).

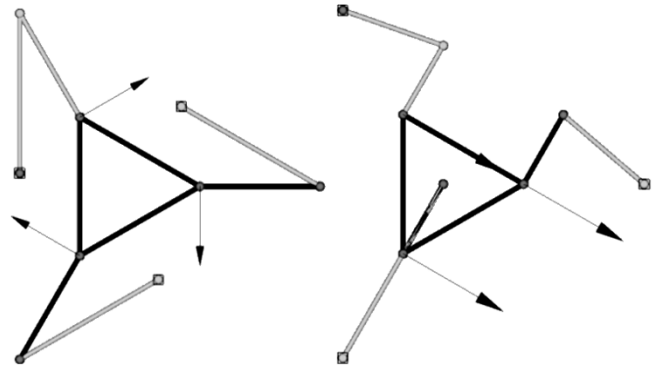


Fig. 6. Uncontrolled motion in DKP configurations.

1) *DKP in the Input*: Rows in the systems (9) or (10), corresponding to the  $F$  kinematic parameters chosen as inputs, are extracted to constitute the system of equations to be analyzed. For example, in planar mechanisms, when dealing with link angular velocities exclusively, the expression extracted from (10) will be as follows:

$$\{\omega_{\text{links}}\}_{Fx1} = [\Omega_{\text{links}}]_{FxF} \{\beta\}_{Fx1} \quad (12)$$

where  $\{\omega_{\text{links}}\}$  is the vector with  $F$  components of link rotations,  $[\Omega_{\text{links}}]$  is the matrix with the correspondent rows from matrix  $[\Omega]$ , and  $\{\beta\}$  are the  $F$  terms. When prismatic pairs are used as inputs, an analogous expression may be used combining equations extracted from (9) or (10).

If the rank of square matrix  $[\Omega_{\text{links}}]$  is less than  $F$ , there is a dependency among the equations in (12) and therefore among the rotations in  $\{\omega_{\text{links}}\}$ . That dependency may be found using standard matrix procedures and will provide as many equations as the rank deficiency of  $[\Omega_{\text{links}}]$  with the form

$$\gamma_1 \omega_{\text{link}1} + \gamma_2 \omega_{\text{link}2} + \dots + \gamma_F \omega_{\text{link}F} = 0. \quad (13)$$

An example may be found in Fig. 1(a), whose DKP equation (6) is found with this method.

If the relationship is among  $r < F$  kinematic parameters, the coefficient  $\gamma_i$  of the parameters not included in the relation will be null. Linkage in Fig. 1(b) is an example, with  $r = 2$  being its DKP relationship (7).

This method will also detect the uncontrolled motion when every input is locked. In this case, (12) is used with the input links set to zero

$$\{\omega_{\text{input}}\} = \{0\} = [\Omega_{\text{input}}] \{\beta\}. \quad (14)$$

As there is a rank deficiency, infinite solutions to the  $\{\beta\}$  terms are obtained in the homogeneous system of (14). Using a proof value for the terms, with (9) and (10) the unexpected motion is found. In Fig. 6, the nodal velocities of the uncontrolled motions in those configurations are shown.

In order to check automatically if the uncontrolled motion involves the end-effector, its kinematic parameters will be analyzed. The components of one nodal velocity and the angular velocity are chosen, and if the  $\beta$  parameters obtained before produce nonzero solutions in (15) the uncontrolled motion involves

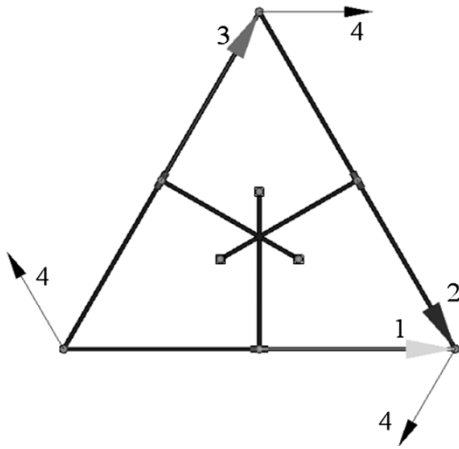


Fig. 7. Vectors of the motion space of a 3-DOF platform in IM.

the end-effector. A higher rank deficiency of (14) produce several sets of  $\beta$  parameters that have to be analyzed

$$\begin{Bmatrix} \{\dot{x}_i\} \\ \{\omega_{\text{platform}}\} \end{Bmatrix} = \begin{bmatrix} V_i \\ \Omega_{\text{platform}} \end{bmatrix} \{\beta\}. \quad (15)$$

2) *DKP in the Output*: The same method is applied to the output kinematic parameters. This method can be applied even when this type of singularity occurs at the same time as an IM singularity. In the position of the 3-RRP planar platform shown in Fig. 7, the linkage is in an IM configuration.

The whole mechanism has an instantaneous DOF equal to four. The motion of the platform can be defined by the velocity in the upper node  $i$  and the angular velocity. If those kinematic parameters are chosen, an expression analogous to (12) is defined as

$$\begin{Bmatrix} \dot{x}_i \\ \dot{y}_i \\ \omega_{z_{\text{platform}}} \end{Bmatrix} = \begin{bmatrix} 0 & 0 & 0 & 1 \\ 0 & 0 & 0 & 0 \\ 0 & 0 & 0 & -1.5 \end{bmatrix} \{\beta\}_{4 \times 1}. \quad (16)$$

Finding the possible dependencies in (16) provides two equations analogous to (13):

$$\begin{aligned} 1.5\dot{x}_i + \omega_{z_{\text{platform}}} &= 0 \\ \dot{y}_i &= 0 \end{aligned} \quad (17)$$

and therefore, the platform has only one DOF. The same may be deduced from the plot of the vectors of the motion space (numbered in Fig. 7), where only eigenvector 4 involves the platform.

3) *LIM*: Finding an equation with  $r = 1$  implies that some kinematic parameter is null whatever the input given. If all of the kinematic parameters that define the motion of a link are null, this link is locked. The method to detect this kind of position is straightforward using (9) or (10). Whenever there is a null row in matrices  $[V]$  or  $[\Omega]$ , the correspondent nodal or angular kinematic parameter is null for any  $\{\beta\}$  terms and, hence, any inputs given. When a link is analyzed, rows correspondent to a node and to the angular velocity of the link are checked. If those rows are null, the link is in LIM in that position independently of the inputs, which is a potential problem in most cases. This analysis provides the user with very useful information when choosing inputs or outputs.

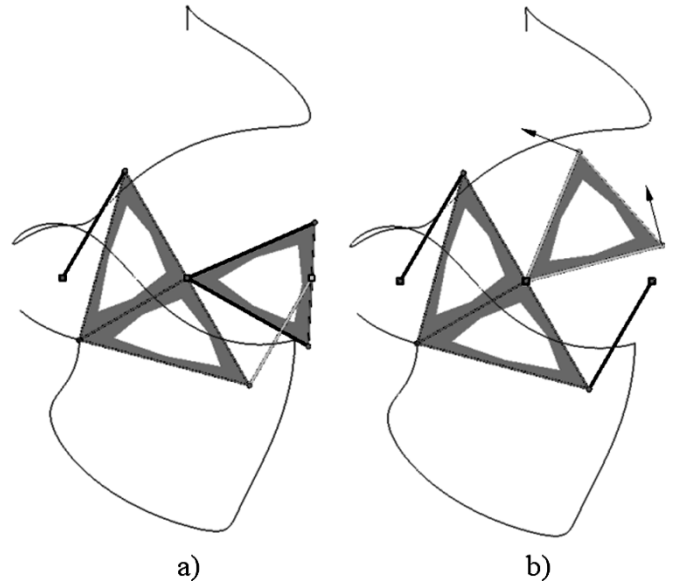


Fig. 8. IM configuration and node velocities in a linkage in a DKP configuration with  $r = 1$ .

If the mechanism in Fig. 5 is moved to the IM configuration corresponding to the lower left bifurcation point [Fig. 8(a)], two possibilities of motion are found. One of them goes on with the motion along the path drawn, but the other one is the motion of part of the linkage while the rest is locked [Fig. 8(b)]. In that case, a DKP configuration with  $r = 1$  happens in the kinematic parameters that define the motion of the locked links.

## V. A PROCEDURE FOR SINGULARITY ANALYSIS

An automatic detection and classification of the singular positions encountered by the mechanism as its motion is simulated has been implemented in computer software developed by this research group. The procedure will allow not only the detection of singularities defined earlier, but will also provide the uncontrolled motions and dependencies that appear.

Even when this procedure will not detect *a priori* every singular configuration of a mechanism, it can be used to find every singular configuration inside the simulated range of motion of the inputs, that is, in the predefined and under-evaluation practical workspace. The automatic capability permits an iterative analysis of different node paths of the linkage, and the inspection of indicators, such as the first nonzero eigenvalue or the rank deficiency of the matrices indicated in the previous section, will point out singularities. A wider iterative process on a discretization of the workspace is feasible and would eventually detect every singularity of the mechanism. However, further research must be done in that sense.

In any event, the process would be as shown in Fig. 9, in every position reached.

For each position, the geometric matrix is found and the eigenvalue problem is solved. Eigenvectors corresponding to null eigenvalues generate matrices  $[V]$  and  $[\Omega]$ .

First, for each link, the kinematic parameters that define its motion are checked. They can be null due to boundary conditions (e.g., a fixed node). But they can also be null due to the special configuration. This is checked in the corresponding row in matrices  $[V]$  and  $[\Omega]$ . In this case, a DKP equation with  $r = 1$

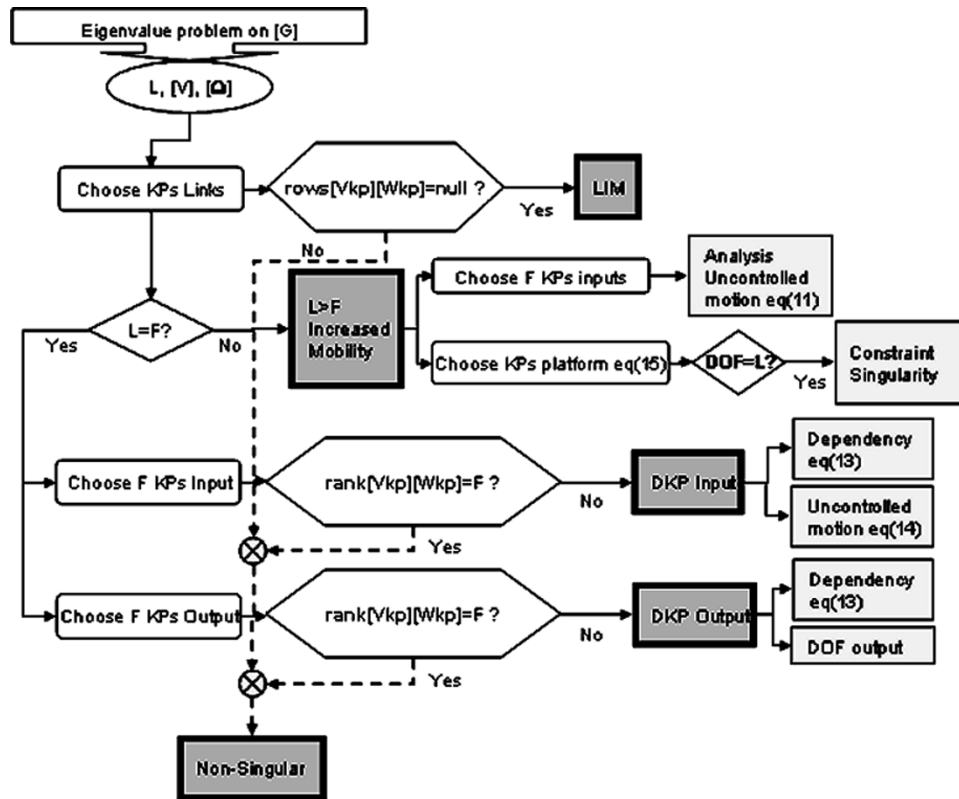


Fig. 9. Algorithm for the singularity detection in a given position.

appears. If all of the kinematic parameters of a link are null, this is in an LIM singular configuration.

Second, an increment in the number of null eigenvalues  $L$  (the instantaneous DOF) over the mobility  $F$  will identify the IM singularity. A further analysis can be done for the  $F$  input links using (11). That solution provides the uncontrollable motion under locked inputs in that configuration. Also, the DOF of the platform may be evaluated choosing the kinematic parameters that define its motion and checking their dependency with equations such as (16). Once this is done, constraint singularities may be detected.

On the other hand, if  $L$  equals  $F$ , there is still the possibility of being in a DKP configuration. To determine these configurations, it is necessary to choose as many kinematic parameters as the DOF. The user can analyze specifically the links that have a greater interest for being either input or output. A complete automatization will need different combinations of links in the linkage covering not only input and output but also passive links.

Once the  $F$  input kinematic parameters have been chosen, depending on their nature, equations like (12) or similar are analyzed. The rank of the matrix of those coefficients  $[\Omega_{links}]$  indicates whether there is a DKP in the input. Those dependencies may be found to get expressions such as (13), and the analysis of the motion when those links are locked may be performed with (14).

The same is performed for the kinematic parameters of the output. In this case, finding the DOF of the output platform is useful.

When links are not in an LIM configuration, the linkage is not in an IM position, and the  $F$  kinematic parameters in the input or output are independent; the linkage is nonsingular.

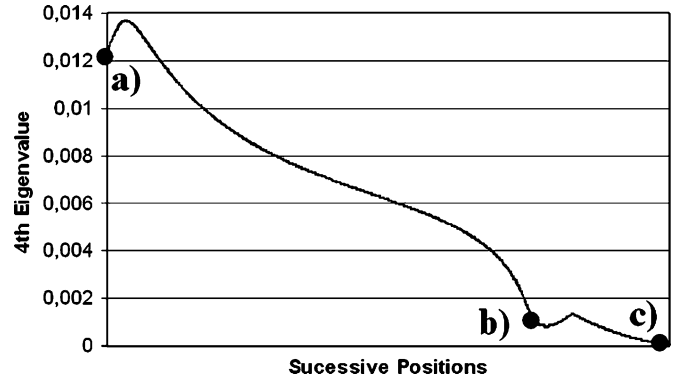


Fig. 10. Graph of the IM indicator along the motion.

A numerical analysis as the one described requires a careful evaluation of the tolerances admitted when considering that an eigenvalue is null or that a rank deficiency occurs. In that sense, the graphs commented in previous sections facilitate the criteria to detect zones where a singularity is likely to happen.

A spatial 3-RSR platform has been analyzed along the motion from a DKP position to the IM configuration. The finite displacement simulation has been performed with the software developed with three inputs in the revolute pairs to ground. The plot of the first nonzero eigenvalue (Fig. 10) indicates how the 3-DOF platform is moving toward a singularity of the IM type. For every simulated successive position, the procedure for singularity detection has been used. Here, three of those positions are explained briefly.

In the first position (Fig. 11), the analysis performed on the kinematic parameters that express the motion in the lower links of each leg signals an LIM. There is no increment in the DOF.

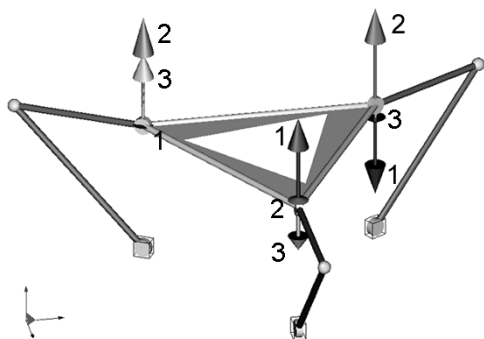


Fig. 11. Position a) showing the three vectors of the motion space numbered and in different shades of color.

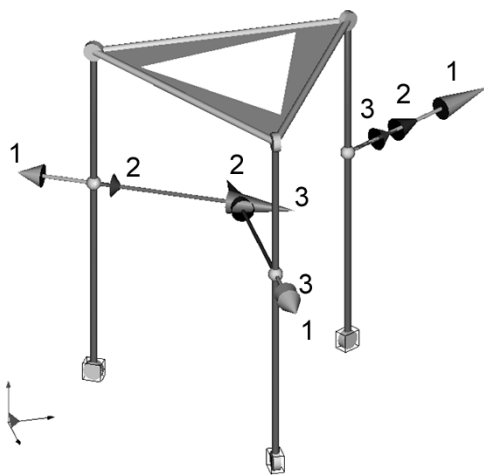


Fig. 12. Position b) with vectors of motion space.

When angular rotations in those links are chosen as inputs, DKP equations with  $r = 1$  show null values. The vectors of the motion space in Fig. 11 are zero in the nodes on the spherical joints of those links, indicating no motion regardless of the input given. An instantaneous uncontrolled motion in the platform occurs. The platform has vertical nodal velocities, and therefore, its angular velocity is on the horizontal plane.

In Fig. 12, the platform reaches its upper position. This time, kinematic parameters that express the motion of the platform signal an LIM configuration. There is no increment in the DOF.

The input kinematic parameters show no dependency. However, the kinematic parameters chosen to represent the motion of the platform (the output) have a DKP equation with  $r = 1$ . Its DOF is found to be zero. No output is obtained, whatever the inputs. Fig. 12 also shows the vectors of the motion space, indicating no motion in any node in the platform.

Finally, in the configuration shown in Fig. 13, the instantaneous DOF of the mechanism is four, and then it is an IM configuration. The uncontrolled motion under locked inputs is found to be a 3-DOF rotation of the platform about point  $A$ . If the six kinematic parameters that represent the platform motion are chosen, the DOF of the platform is found to be four: three rotations and one translation. Therefore, a constraint singularity occurs in this position.

The procedure as it is implemented allows the singularity analysis of simulated paths. Once singularities are detected, the system offers information that can be used to avoid uncontrolled motions or to change inputs. IM proximity is evaluated with a graph that serves also as a platform stability index.

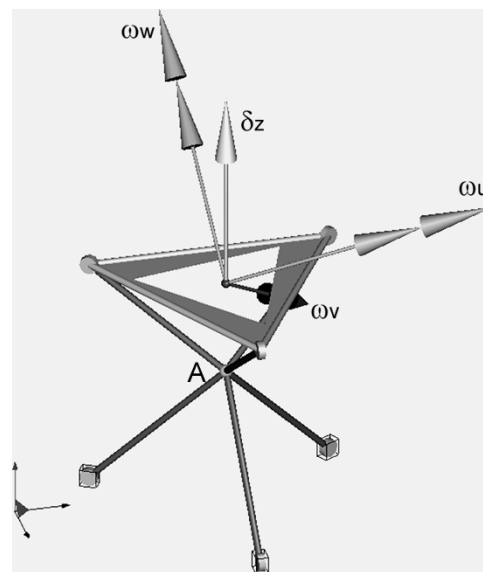


Fig. 13. Position c), IM configuration with the vectors of the four DOF of the platform.

## VI. DISCUSSION

Nowadays, there are roughly three methods in the search for singularities: degeneracy of the screws (alternatively Grassmann line geometry), algebraic methods, and numerical approaches. Symbolic computation may be combined with them to facilitate the solution.

The first one seems to be the quickest and most efficient, at least in the finding of the geometric relationships that produce a singularity. The problem is that there is an additional task. It is necessary to find the position that accomplishes those conditions in the workspace. Besides, the procedure requires a good knowledge of the kinematic geometry of the manipulator. All of this implies that the method is strongly dependent on the abilities of the kinematician and, hence, the possibilities for automatization are scarce. Less advantages and the same restrictions apply to algebraic methods. Finding the geometrical conditions of singularity is a complex issue. Later, those conditions have to be used to find the singular configuration. Nevertheless, we have not discarded the analytical way. In fact, some ideas are under evaluation. Instead of looking for the roots of the Jacobian, our approach will be to work on the polynomial equation of the eigenvalues of the geometric matrix using symbolic computation.

However, in the area we are focusing on, a greater effort is in the numerical approach. This is the most laborious and requires a higher computational cost. However, this research team has some experience in the numerical analysis of mechanical problems and believes that it is worth trying. There are some good reasons for that. The procedure described in this paper is the starting point for the singularity mapping. We have also created a very efficient program for the solving the forward and inverse position problem of any manipulator (not described in the paper). The strategy is to mesh the workspace into cells and apply adaptive refinement techniques using the first nonzero eigenvalue as an indicator of IM singularities. Other indicators, such as singular values, are also under evaluation. The fact that the geometric matrix equation is a homogeneous equation in terms of linear velocities is an important issue here.

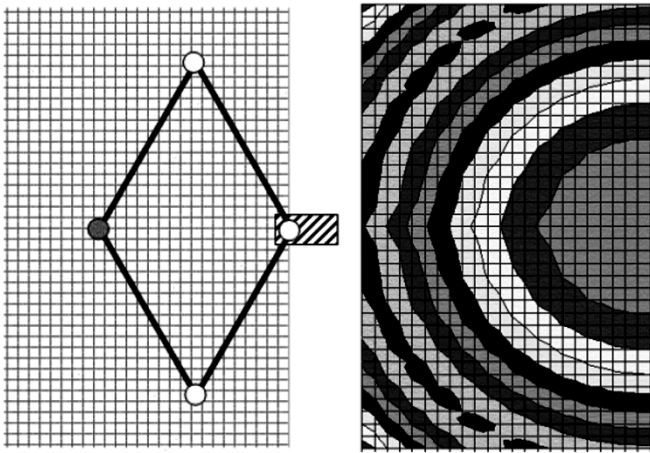


Fig. 14. 2RR planar platform and IM indicator.

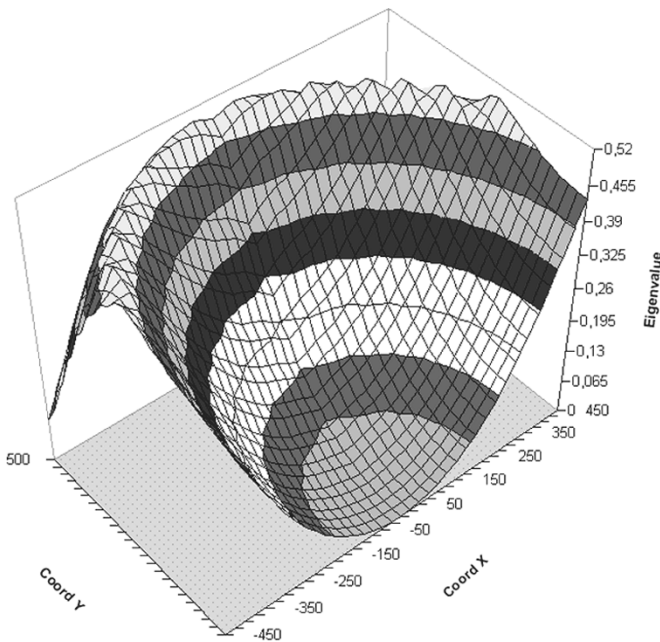


Fig. 15. Three-dimensional plot of the IM indicator.

A preliminary example is given in Fig. 14. The 2-DOF planar platform 2RR with equal lengths in every link is analyzed in a given area. A plot of the IM indicator in that area shows the existence of an IM singularity when the end-effector is on the origin (see Figs. 14 and 15). A variant of the same example is given in Fig. 16(a). The 2RR platform is analyzed in a given area. The plot of the DKP input indicator in the meshed area [see Fig. 16(b)] shows the existence of a singularity exactly in the position of the linkage shown in Fig. 16(a). For the sake of clarity, numerical values are not included in the plot, but there is a zone A where these are very close to zero. A finer mesh is required here until exact positions of DKP configurations are found. However, in practical applications, it is often enough to mark an area of singularities. In Fig. 16(c), a plot of DKP singularity in the output is shown. In zone B, the values are close to zero and an area of this type of singularity is delimited.

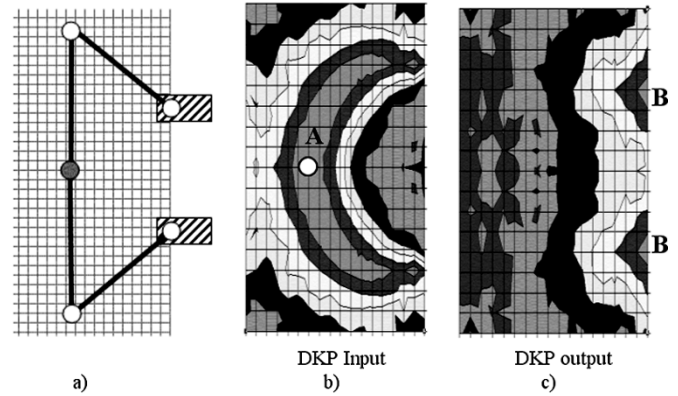


Fig. 16. 2RR platform along the DKP indicators in the input and output.

Further research is needed in this field in order to reduce computational costs and optimize tolerance criteria. In every location of the platform, there are different possible configurations that produce different values of the indicators. This is also an open issue. Finally, this has to be extended to spatial parallel manipulators. For the time being, these are the open lines in our research in the field of singularities.

## VII. CONCLUSION

We have presented a practical method to detect and classify singular positions that is easy to automate for any linkage. As a consequence, an algorithm for singularity detection and analysis has been implemented in a software for mechanisms. There are promising features for an automatic singularity analysis not only of planar, but also spatial, mechanisms and redundant and nonredundant linkages.

The use of the vectors of the motion space provides the DOF associated with the singularity configuration of the linkage or the platform, dependencies among kinematic parameters, and uncontrollable motions in singular positions. Two types of singularities have been described; increased mobility IM and DKP configurations. Constraint singularities can be analyzed using this procedure.

## APPENDIX

In order to show the simplicity to form the velocity equation in a mechanism using the geometric matrix, a simple example, as shown in Fig. 17, will be presented.

From the rigid body condition between the nodes  $i$  and  $j$  sited on the extremes of a link

$$L^2 = \{x_i \ y_i \ x_j \ y_j\} \times \begin{bmatrix} \cos^2 \theta & \cos \theta \sin \theta & -\cos^2 \theta & -\cos \theta \sin \theta \\ \cos \theta \sin \theta & \sin^2 \theta & -\cos \theta \sin \theta & -\sin^2 \theta \\ -\cos^2 \theta & -\cos \theta \sin \theta & \cos^2 \theta & \cos \theta \sin \theta \\ -\cos \theta \sin \theta & -\sin^2 \theta & \cos \theta \sin \theta & \sin^2 \theta \end{bmatrix} \times \begin{Bmatrix} x_i \\ y_i \\ x_j \\ y_j \end{Bmatrix} \quad (A1)$$

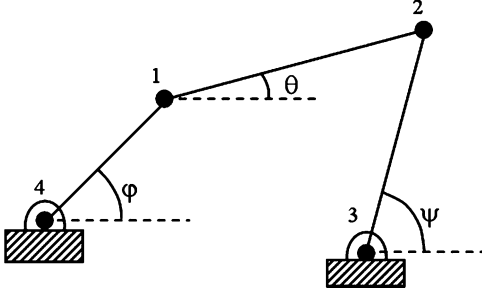


Fig. 17. A four-bar planar linkage.

a matrix equation for velocities in the link is deduced using differentiation

$$[g]_e \{\dot{x}\}_e = \{0\} \quad (\text{A2})$$

where  $[g]_e$  is the geometric matrix of the element  $e$  and has the data related to bar orientation but is independent of its length, section, or other mechanical properties. For a bar link 1–2 in planar motion, the geometric matrix equation is

$$[g]_{12} \{\dot{x}\}_{12} = \begin{bmatrix} \cos^2 \theta & \cos \theta \sin \theta & -\cos^2 \theta & -\cos \theta \sin \theta \\ \cos \theta \sin \theta & \sin^2 \theta & -\cos \theta \sin \theta & -\sin^2 \theta \\ -\cos^2 \theta & -\cos \theta \sin \theta & \cos^2 \theta & \cos \theta \sin \theta \\ -\cos \theta \sin \theta & -\sin^2 \theta & \cos \theta \sin \theta & \sin^2 \theta \end{bmatrix} \times \begin{Bmatrix} \dot{x}_1 \\ \dot{y}_1 \\ \dot{x}_2 \\ \dot{y}_2 \end{Bmatrix}. \quad (\text{A3})$$

Note that, if preferred, the geometric matrix may be expressed in terms of the coordinates of the bar nodes and length. In fact, for spatial mechanisms, the geometric matrix for a rod element (no rotational DOF on its axis) is expressed more easily in that way, as shown in (A4), given at the bottom of the page, where  $\Delta x = x_2 - x_1$ ,  $\Delta y = y_2 - y_1$ , and  $\Delta z = z_2 - z_1$ .

In order to find velocities for every node in the linkage, an expansion of (A2) to the total number of Cartesian coordinates in the mechanism will be carried out. If the mechanism has  $n$  nodes, the number of nodal coordinates for a planar mechanism will be  $2n$ . Also, the geometric matrix expanded to the whole mechanism will have an order  $2n \times 2n$ , in which the terms of the geometric matrix of the bar link with an order  $4 \times 4$  will be placed in rows and columns  $2i - 1$ ,  $2i$ ,  $2j - 1$ , and  $2j$ , the rest being zero. If the mechanism is formed by  $M$  bar links, there are  $M$  matrix equations like (A3). In the linkage of the example, there are three such equations.

A link of the mechanism is subjected to constraints in position and velocity imposed by the rest of the links. This is imposed upon assembling of these expanded matrices, and, as a consequence, the geometric matrix for the complete mechanism is found and is given in (A5), shown at the bottom of the page.

Now, it is possible to include the constraints imposed by joints to the fixed element, and therefore, the complete velocity equation may be expressed as (A6), shown at the top of the next page, and will provide the solution to the kinematic analysis. Boundary conditions, such as fixed joints or sliding blocks, are introduced using the equations that relate nodal velocities of those joints.

$$[g] \{\dot{x}\}_{12} = \frac{1}{L_{12}^2} \begin{bmatrix} \Delta^2 x & \Delta x \Delta y & \Delta x \Delta z & -\Delta^2 x & -\Delta x \Delta y & -\Delta x \Delta z \\ \Delta x \Delta y & \Delta^2 y & \Delta y \Delta z & -\Delta x \Delta y & -\Delta^2 y & -\Delta y \Delta z \\ \Delta x \Delta z & \Delta y \Delta z & \Delta^2 z & -\Delta x \Delta z & -\Delta y \Delta z & -\Delta^2 z \\ -\Delta^2 x & -\Delta x \Delta y & -\Delta x \Delta z & \Delta^2 x & \Delta x \Delta y & \Delta x \Delta z \\ -\Delta x \Delta y & -\Delta^2 y & -\Delta y \Delta z & \Delta x \Delta y & \Delta^2 y & \Delta y \Delta z \\ -\Delta x \Delta z & -\Delta y \Delta z & -\Delta^2 z & \Delta x \Delta z & \Delta y \Delta z & \Delta^2 z \end{bmatrix} \begin{Bmatrix} \dot{x}_1 \\ \dot{y}_1 \\ \dot{z}_1 \\ \dot{x}_2 \\ \dot{y}_2 \\ \dot{z}_2 \end{Bmatrix} \quad (\text{A4})$$

$$[G] = \sum_{i=1}^M [\bar{g}]_e = \begin{bmatrix} c^2 \theta + c^2 \varphi & c \theta s \theta + c \varphi s \varphi & -c^2 \theta & -c \theta s \theta & 0 & 0 & -c^2 \varphi & -c \varphi s \varphi \\ c \theta s \theta + c \varphi s \varphi & s^2 \theta + s^2 \varphi & -c \theta s \theta & -s^2 \theta & 0 & 0 & -c \varphi s \varphi & -s^2 \varphi \\ -c^2 \theta & -c \theta s \theta & c^2 \theta + c^2 \varphi & c \theta s \theta + c \varphi s \varphi & -c^2 \varphi & -c \varphi s \varphi & 0 & 0 \\ -c \theta s \theta & -s^2 \theta & c \theta s \theta + c \varphi s \varphi & s^2 \theta + s^2 \varphi & -c \varphi s \varphi & -s^2 \varphi & 0 & 0 \\ 0 & 0 & -c^2 \varphi & -c \varphi s \varphi & c^2 \varphi & c \varphi s \varphi & 0 & 0 \\ 0 & 0 & -c \varphi s \varphi & -s^2 \varphi & c \varphi s \varphi & s^2 \varphi & 0 & 0 \\ -c^2 \varphi & -c \varphi s \varphi & 0 & 0 & 0 & 0 & c^2 \varphi & c \varphi s \varphi \\ -c \varphi s \varphi & -s^2 \varphi & 0 & 0 & 0 & 0 & c \varphi s \varphi & s^2 \varphi \end{bmatrix} \quad (\text{A5})$$

$$\begin{bmatrix} c^2\theta + c^2\varphi & c\theta s\theta + c\varphi s\varphi & -c^2\theta & -c\theta s\theta & 0 & 0 & 0 & 0 \\ c\theta s\theta + c\varphi s\varphi & s^2\theta + s^2\varphi & -c\theta s\theta & -s^2\theta & 0 & 0 & 0 & 0 \\ -c^2\theta & -c\theta s\theta & c^2\theta + c^2\psi & c\theta s\theta + c\psi s\psi & 0 & 0 & 0 & 0 \\ -c\theta s\theta & -s^2\theta & c\theta s\theta + c\psi s\psi & s^2\theta + s^2\psi & 0 & 0 & 0 & 0 \\ 0 & 0 & 0 & 0 & 1 & 0 & 0 & 0 \\ 0 & 0 & 0 & 0 & 0 & 1 & 0 & 0 \\ 0 & 0 & 0 & 0 & 0 & 0 & 1 & 0 \\ 0 & 0 & 0 & 0 & 0 & 0 & 0 & 1 \end{bmatrix} \begin{Bmatrix} \dot{x}_1 \\ \dot{y}_1 \\ \dot{x}_2 \\ \dot{y}_2 \\ \dot{x}_3 \\ \dot{y}_3 \\ \dot{x}_4 \\ \dot{y}_4 \end{Bmatrix} = \{0\} \quad (\text{A6})$$

This review is performed for bar elements. However, any link of a higher order (e.g., tertiary or quaternary) may be modeled by bars connected with revolute pairs. Anyway, developing specific geometric matrices for those links is also an alternative approach.

#### REFERENCES

- [1] K. Sugimoto, J. Duffy, and K. H. Hunt, "Special configurations of spatial mechanisms and robot arms," *Mech. Mach. Theory*, vol. 17, no. 2, pp. 119–132, 1982.
- [2] J. Angeles and A. Bernier, "A general method of four bar linkage mobility analysis," *Trans. ASME J. Mech. Transmission Automat. Des.*, vol. 109, no. 2, pp. 197–203, 1987.
- [3] K. H. Hunt, "Special configurations of robot arms via screw theory," *Robotica*, vol. 4, pp. 171–179, 1986.
- [4] G. Schreiber, M. Otter, and G. Hirzinger, "Solving the singularity problem of nonredundant manipulators by constraint optimization," in *Proc. IEEE/RSJ Int. Conf. Intelligent Robots and Systems*, Kyongju, Korea, 1999, pp. 1482–1488.
- [5] J.-P. Merlet, "Singular configurations of parallel manipulators and Grassmann geometry," *Int. J. Robot. Res.*, vol. 8, no. 5, pp. 45–56, 1989.
- [6] A. Karger and M. Husty, "Classification of all self-motions of the original Stewart–Gough platform," *Computer-Aided Des.*, vol. 30, no. 3, pp. 205–215, 1998.
- [7] R. Di Gregorio and V. Parenti-Castelli, "Mobility analysis of the 3-UPU parallel mechanism assembled for a pure translational motion," in *Proc. IEEE/ASME Int. Conf. Advanced Intelligent Mechatronics*, Atlanta, GA, 1999, pp. 520–525.
- [8] I. Bonev, "Geometric analysis of parallel mechanisms," Ph.D. dissertation, Laval Univ., Quebec, QC, Canada, 2002.
- [9] D. S. Zlatanov, R. G. Fenton, and B. Benhabib, "Analysis of the instantaneous kinematics and singular configurations of hybrid-chain manipulators," *Robot.: Kinemat., Dynam. Controls*, vol. 72, pp. 467–476, 1994.
- [10] D. S. Zlatanov, R. G. Fenton, and B. Benhabib, "Classification and interpretation of the singularities of redundant mechanisms," in *Proc. ASME Design Engineering Tech. Conf.*, Atlanta, GA, 1998, pp. 1–11.
- [11] D. S. Zlatanov, I. A. Bonev, and C. M. Gosselin, "Constraint singularities as c-space singularities," in *Advances in Robot Kinematics. Theory and Applications*. Dordrecht, The Netherlands: Kluwer, 2002.
- [12] O. Ma and J. Angeles, "Architecture singularities of parallel manipulators," *Int. J. Robot. Automat.*, vol. 7, no. 1, pp. 23–29, 1992.
- [13] L. Notash, "Uncertainty configurations of parallel manipulators," *Mech. Mach. Theory*, vol. 33, no. 1/2, pp. 123–138, 1998.
- [14] F. C. Park and J. W. Kim, "Singularity analysis of closed kinematic chains," *ASME J. Mech. Des.*, vol. 121, pp. 32–38, 1999.
- [15] K. H. Hunt, *Kinematic Geometry of Mechanisms*. Oxford, U.K.: Clarendon, 1978.
- [16] C. Gosselin and J. Angeles, "Singularity analysis of closed-loop kinematic chains," *IEEE Trans. Robot. Automat.*, vol. 6, pp. 281–290, June 1990.
- [17] D. Zlatanov, R. G. Fenton, and B. Benhabib, "Singularity analysis of mechanisms and robots via velocity-equation model of the instantaneous kinematics," in *Proc. IEEE Int. Conf. Robotics and Automation*, vol. 2, 1994, pp. 986–991.
- [18] V. Kumar, "Characterization of workspaces of parallel manipulators," *Trans. ASME J. Mech. Des.*, vol. 114, pp. 368–375, 1992.
- [19] J.-P. Merlet, *Parallel Robots*. Dordrecht, The Netherlands: Kluwer, 2000.
- [20] D. Zlatanov, R. G. Fenton, and B. Benhabib, "Identification and classification of the singular configurations of mechanisms," *Mech. Mach. Theory*, vol. 33, no. 6, pp. 743–760, 1998.
- [21] F. Freudenstein, "On the variety of motions generated by mechanisms," *Trans. ASME J. Eng. Ind.*, pp. 156–160, Feb. 1962.
- [22] A. Hernández, O. Altuzarra, R. Avilés, and V. Petuya, "Kinematic analysis of mechanisms via a velocity equation based in a geometric matrix," *Mech. Mach. Theory*, vol. 38, no. 12, pp. 1413–1429, 2003.
- [23] B. Paul, *Kinematics and Dynamics of Planar Machinery*. Englewood Cliffs, NJ: Prentice-Hall, 1979.
- [24] D. Zlatanov, R. G. Fenton, and B. Benhabib, "A unifying framework for classification and interpretation of mechanism singularities," *J. Mech. Des.*, vol. 117, pp. 566–572, 1995.



mechanical problems.

**Oscar Altuzarra** was born in 1971. He received the M.Sc. and Ph.D. degrees in mechanical engineering from the University of the Basque Country (UPV/EHU), Bilbao, Spain, in 1995 and 1999, respectively.

Since 1996, he has been a Lecturer and then Associate Professor with the Department of Mechanical Engineering, Engineering School of Bilbao, UPV/EHU. His research interests are kinematics and singularities in parallel kinematic machines, robotics, and computational applications to complex



workspace and prototypes in PKM, computational mechanics, and analysis of the discretization error in nonlinear structural problems via FEM.

**Charles Pinto** received the degree in mechanical engineering from the Faculty of Engineering in Valenciennes (ENSIMEV), Valenciennes, France, in 1993, the D.E.A. in mechanical design from the University of Valenciennes (UVHC), Valenciennes, France, in 1994, and the Ph.D. degree in mechanical engineering from the University of the Basque Country (UPV/EHU), Bilbao, Spain, in 2001.

He is an Associate Professor with the Department of Mechanical Engineering, Faculty of Engineering, UPV/EHU. His research interests are kinematics,



**Rafael Avilés** was born in 1954. He received the M.Sc. and Ph.D. degrees in mechanical engineering from the University of the Basque Country (UPV/EHU), Bilbao, Spain, in 1976 and 1980, respectively.

In 1977, he became a Lecturer with the School of Engineering, UPV/EHU. In 1984, he became a Professor with the Mechanical Engineering Department, and he was its Director from 1984 to 1991. He has published over one hundred papers in journals and international congresses. At present, his research activities

are in the field of design and analysis of multibody systems and mechanisms, specifically adaptative variable geometry trusses and fatigue effects in those components.



**Alfonso Hernández** received the M.Sc. and Ph.D. degrees in mechanical engineering from the University of the Basque Country (UPV/EHU), Bilbao, Spain, in 1985 and 1988, respectively.

He has developed lecture and research activities at UPV/EHU, where he has been a Professor of Mechanical Engineering since 1995. He has had educational material published in the fields of machine theory, machine design, and theory of vibrations. In addition, for lecture (and research) purposes, he has designed various computer programs for the analysis

and design of mechanisms. He has had numerous papers published in refereed journals in the fields of reliability of the finite-element method, nonlinear structural problems, and mechanisms. Currently he is leading two separate research projects: Advanced Mechanical Design and Analysis, and New Analysis Techniques for the Design of Parallel Kinematic Manipulators.